



Universiteit
Leiden
The Netherlands

Chitin in the fungal cell wall: Towards valorization of spent biomass of *Aspergillus niger*

Leeuwe, T.M. van

Citation

Leeuwe, T. M. van. (2020, November 4). *Chitin in the fungal cell wall: Towards valorization of spent biomass of Aspergillus niger*. Retrieved from <https://hdl.handle.net/1887/138011>

Version: Publisher's Version

License: [Licence agreement concerning inclusion of doctoral thesis in the Institutional Repository of the University of Leiden](#)

Downloaded from: <https://hdl.handle.net/1887/138011>

Note: To cite this publication please use the final published version (if applicable).

Cover Page



Universiteit Leiden



The handle <http://hdl.handle.net/1887/138011> holds various files of this Leiden University dissertation.

Author: Leeuwe, T.M. van

Title: Chitin in the fungal cell wall: Towards valorization of spent biomass of *Aspergillus niger*

Issue date: 2020-11-04

CHAPTER 6

Deletion of the *Aspergillus niger* pro-protein processing protease gene *kexB* results in a pH-dependent morphological transition during submerged cultivations and increases cell wall chitin content

Tim M. van Leeuwe, Mark Arentshorst, Gabriel Forn-Cuní, Nicholas Geoffrion, Adrian Tsang, Frank Delvigne, Annemarie H. Meijer, Arthur F.J. Ram, Peter J. Punt

ABSTRACT

There is a growing interest for the use of post-fermentation mycelial waste to obtain cell wall chitin as an added-value product. In the pursuit to identify suitable production strains that can be used for post-fermentation cell wall harvesting, we turned to an *Aspergillus niger* strain in which the *kexB* gene was deleted. Previous work has shown that deletion of *kexB* causes hyper-branching and thicker cell walls, traits that may be beneficial for reduction of fermentation viscosity and lysis. Hyper-branching of $\Delta kexB$ was previously found to be pH-dependent on solid medium at pH 6.0, but was absent at pH 5.0. This phenotype was reported to be less pronounced during submerged growth. Here, we show a series of controlled batch cultivations at a pH range of 5, 5.5, and 6 to examine the pellet phenotype of $\Delta kexB$ in liquid medium. Morphological analysis showed that $\Delta kexB$ formed wild type-like pellets at pH 5.0 whereas the hyper-branching $\Delta kexB$ phenotype was found at pH 6.0. Transition of phenotypic plasticity was found in cultivations at pH 5.5, seen as an intermediate phenotype. Analyzing the cell walls of $\Delta kexB$ from these controlled pH-conditions showed an increase in chitin content compared to wild type across all three pH values. Surprisingly, the increase in chitin content was found to be irrespective of the hyper-branching morphology. Evidence for alterations in cell wall make-up are corroborated by transcriptional analysis that showed a significant cell wall stress response in addition to upregulation of genes encoding other unrelated cell wall biosynthetic genes.

Manuscript submitted

1. INTRODUCTION

Filamentous fungi are industrially used to produce a range of products, from organic acids, antibiotics and other metabolites to enzymes and (heterologous) proteins. However, the industrial scale fermentation using filamentous fungi is typically limited by limited oxygen supply due to the high viscosity of the fermentation broth at high mycelial growth densities. These conditions impair homogeneous mixing, are very energy demanding, and cause stress to the fungus due to the high amounts of hyphal shearing. Fluctuation in nutrient and oxygen levels caused by sub-optimal mixing within the large scale fermentation vessels can subsequently lead to additional metabolic stress and shifts, diminishing batch-to-batch consistency and product quality (Cai et al., 2014; Papagianni, 2004).

In addition to high viscosity problems, intensive use of filamentous fungi as cell factories at an industrial scale produces large amounts of spent mycelium left over as a by-product. Spent mycelium has been suggested to be a source of chitin and chitosan products by extracting this from the fungal cell wall to be used for many applications in medicine and agriculture (Dhillon et al., 2012; Naveed et al., 2019; Orzali et al., 2017). To both outcompete the current supply of chitin from crustacean shell waste and to make chitin yields a profitable option, optimization of extraction and high chitin levels are required (Cai et al., 2006; Dhillon et al., 2012). Efforts have been made do so by genetic modification of the chitin biosynthetic pathway or through alterations of fermentation conditions (Deng et al., 2005; Hammer and Carr, 2006; Ja'afaru, 2013; Nwe and Stevens, 2004). Additionally, we recently reported on the identification of two *Aspergillus niger* UV-mutants that showed increased cell wall chitin (van Leeuwe et al., 2020b, 2020a). These efforts contribute to explore the use of spent mycelium as an added-value product rather than waste output.

In the endeavor to address both the issue of fermentation (mycelial) viscosity and increase chitin production, we turned to an *A. niger kexB* deletion strain that is already known for impaired pro-protein processing. A deletion of *kexB* has already been shown to be beneficial for secretion of fusion proteins consisting of a well secreted carrier and proteolytically sensitive proteins (Punt et al., 2003). In *A. niger*, *kexB* (also named *pclA* in literature) was shown to be implicated in the processing of dibasic cleavage sites of secretory proteins (Jalving et al., 2000, Punt et al., 2003). The *A. niger* KexB protein is the homologue of *Saccharomyces cerevisiae* Kex2p, a Ca²⁺-dependent serine protease that is responsible for processing dibasic Lys-Arg or Arg-Arg cleavage sites for maturation of secreted proteins (Fuller et al., 1989). Designated proteins that pass through the secretory pathway are processed in the Golgi apparatus where kexin proteins reside due to their Golgi-retention signal (Bryant and Stevens, 1997; Wilcox and Fuller, 1991). These Kex enzymes are important in ascomycete alpha-pheromone processing (Le Marquer et al., 2019; Martin et al., 2011), first discovered in yeast, where 2 to 4 copies of the alpha-pheromone are processed into peptides by *kex2* (Achstetter, 1989; Leibowitz and Wickner, 1976; Wagner and Wolf, 1987). Additionally, Kex2 was shown to be important in subsequent steps of mating during cell fusion

(Heiman et al., 2007). Furthermore, in filamentous fungi, KexB is implicated in the processing of cyclic and modified peptides (Ding et al., 2016; Nagano et al., 2016). Previous reports have also shown that the *A. niger* $\Delta kexB$ strain displayed shorter, visibly thicker hyphae and a hyperbranching morphology (Jalving et al., 2000; Punt et al., 2003; te Biesebeke et al., 2005). Shorter hyphae and smaller pellets are ideal traits in order to reduce stirring viscosity in fermenter conditions, but the actual performance of this strain under fermentation conditions has not been fully explored. Also, cell wall compositional assessments have never been performed in any *kexB* mutant strain in *A. niger*. Besides the above-mentioned processing targets of yeast and fungal kexins, many more putatively kexin-processed proteins can be found in fungal proteomes and inferred from the corresponding genomes.

A knockout of *KEX2* in *Candida albicans* resulted in reduced virulence with an acclaimed 147 putatively predicted proteins that were identified as potential Kex2p targets that relate to cell wall construction and modification, including hydrolases, adhesins, cell wall components, and outer membrane proteins (Newport et al., 2003). Previous work in *A. oryzae* has also shown that deletion of *kexB* affects cell wall synthesis and activation of the CWI pathway by MAPK phosphorylation assays (Mizutani et al., 2016, 2004; te Biesebeke et al., 2005). Using Prediction algorithms such as ProP (v.1.0b ProPeptide Cleavage Site Prediction), a plethora of putative KexB targets can be identified which are only indicative for potential targets and lack biological interpretation of any relation to the observed pleiotropic effects, such as shorter hyphae and a hyperbranching phenotype. Interestingly, this growth phenotype has clearly been shown on plates at pH 6.0, but not at pH 5.0, suggesting a pH-dependent phenotype (Jalving, 2005), but a detailed study how the $\Delta kexB$ strain behaves during submerged growth is lacking. Here, we investigated the role of KexB on hyphal morphology in pH-controlled batch cultivations. In doing so, we aimed to investigate the impact of deleting *kexB* in *A. niger* on the cell wall composition with respect to its shorter and thicker hyphae.

2. MATERIALS AND METHODS

2.1 Strains, media, growth conditions

Strains used in this study can be found in Table 1. All media were prepared as described by Arentshorst et al., 2012. In all cases, minimal medium (MM) contained 1% (w/v) glucose, 1.5% agar (Scharlau, Barcelona, Spain) and was not supplemented unless otherwise specified. Complete medium (CM) contained 0.1% (w/v) casamino acids and 0.5% (w/v) yeast extract in addition to MM. Strains were inoculated from -80°C glycerol stocks onto fresh CM plates and were allowed to grow and sporulate for 5-7 days at 30°C, prior to spore harvesting. Spores were harvested by addition of 15 mL of 0.9% (w/v) NaCl to CM spore plates and were carefully scraped from the surface with a cotton swab. In case of harvesting spore plates for bioreactor cultivations, 0.05% Tween-80 was added to the 0.9% (w/v) NaCl to prevent spore clumping. Spore solutions were poured over sterile cotton filters (Amplitude™ Ecocloth™ Wipes, Contec Inc., Spartanburg,

SC, USA) to remove large mycelial debris. Spore solutions were counted using Bio-Rad TC20™ Automated Cell Counter (Bio-Rad Laboratories, Inc. USA) using Counting Slides, Dual Chamber for Cell Counter (Cat#145-0011, Bio-Rad Laboratories, Inc. USA).

Table 1. All strains used in this study

Name	Genotype	Reference
N402	cspA1	Bos et al., 1988
AB4.1Δ <i>pclA</i>	cspA1, <i>pyrG</i> , Δ <i>kexB::AOpyrG</i>	Punt et al., 2003
MA234.1	cspA1, Δ <i>kusA::DR-amdS-DR</i>	Park et al., 2016
TLF39	cspA1, Δ <i>kusA::DR-amdS-DR</i> , Δ <i>crhA-G</i>	van Leeuwe et al., 2019
TLF69	cspA1, Δ <i>kusA::DR-amdS-DR</i> , Δ <i>crhA-G</i> , Δ <i>kexB::hygB</i>	This study

2.2 Bioreactor cultivation

Controlled batch cultivations for *A. niger* strains N402 and the Δ*kexB* strain were performed in 6.6L BioFlo bioreactors (New Brunswick Scientific), as previously described (Jørgensen et al., 2010). A batch of 21 L MM containing 0.75% D-glucose was made by adding 1 L filter-sterilized (0.2 μm pore) glucose (15.75% w/v) solution to a freshly autoclaved volume of 20 L MM (no carbon source) as described above. Allowing 1 day of dissolving and a check for contamination, 5 L MM 0.75% glucose was added to each bioreactor directly after autoclaving. Temperature, acidity and stir speed were set to and kept at 30°C, pH 3 and 250 rpm, respectively. The pH was controlled by addition of titrants (2M NaOH and 1M HCl). Sparger aeration of 1 L/min was left on to allow oxygen saturation of the medium prior to inoculation. Next, aeration was set to headspace only and 1.5 mL 10% w/v Yeast Extract was added to the medium to promote homogeneous germination for the to-be-added spores. Subsequently, a total of 5×10^9 (10^6 sp/mL) spores were added to the medium using a concentrated spore solution. Germination time of approximately 4-5h was maintained, preceding the addition of polypropylene glycol P2000 anti-foam agent, increasing agitation to 750 rpm and changing aeration from headspace to sparger only (1 L/min). Oxygen, base and acid consumption were monitored and samples were taken at regular intervals to obtain biomass, culture filtrate and microscopy samples. Biomass was harvested by applying a vacuum over Whatman™ Glass Microfiber Filter (GF/C™) (diameter 47 mm, CAT No.1822-047, Buckinghamshire, UK). Samples were all quickly frozen in liquid nitrogen prior to storage at -80°C. Biomass accumulation through time was gravimetrically determined by lyophilizing designated samples from the corresponding broth culture mass.

2.3 Biofilm cultivations

Biofilm cultivations were performed in a 4 stirred-tank mini-bioreactors platform (DASGIP DASbox Reactor SR0250ODLS, Eppendorf AG, Hamburg, Germany). For promoting biofilm formation, stirring device was completely removed in order to leave space to two sheets of stainless-steel 316L wire gauze. These metal sheets were used as support promoting biofilm growth. Each bioreactor was filled with 200 mL of MM and operated at 30°C. The pH level was maintained

at 5 or 6 depending on the experiment (controlled by the addition of NH_4OH or H_3PO_4) and the air flow rate was adjusted to 200 mL/min. Dissolved oxygen was measured using PSt1 optical sensors linked to an OXY-4 oxygen meter (Presens Precision Sensing, Regensburg, Germany). Each bioreactor was initially inoculated with spores in order to reach 10^6 sp/mL. At the end of the cultivation, metal sheets were removed from the bioreactor for estimating the biofilm wet (in this case, the sheets were left for 30 minutes in a beaker for removing excess of liquid before mass measurement) and dry (estimated after keeping the sheets at 105°C for 24 hours) weight.

2.4 Microscopy

Pellet morphology samples were taken at 100% biomass and visualized in a Zeiss Observer confocal laser-scanning microscope (Zeiss, Jena, Germany). Images were processed and analyzed using FIJI (ImageJ) software (Schindelin et al., 2012).

2.5 Cell wall isolation and chitin analysis

Cell wall samples were isolated as previously described (van Leeuwe et al., 2020b). In short, dried mycelium was frozen in liquid N_2 and were ground to break open the cells. Samples were washed to remove intracellular debris and proteins, three times with 1M NaCl and three times with MilliQ ultrapure water (MQ). Supernatant was carefully discarded prior to the next washing step. Cell wall samples were lyophilized after washing steps for 48h. Cell wall isolation, hydrolysis and chitin content analysis, measured as total glucosamine, have been performed as described previously (van Leeuwe et al., 2020b). Cell wall glucosamine measurements from independent replicate experiments are expressed as means \pm SE.

2.6 RNA isolation and RNA-sequencing

RNA was isolated from mycelial biomass samples obtained from batch cultivated *A. niger* strains N402 and $\Delta pclA$ ($\Delta kexB$), using TRIzol (Invitrogen). RNA was purified afterwards with NucleoSpin RNA Clean-up kit (Macherey-Nagel) with DNase treatment. Concentration and quality of the RNA was determined using a NanoDrop 2000 spectrophotometer (Thermo Scientific) and by gel-electrophoresis, respectively. RNA sample were sent to Genome Québec for sequencing using the HiSeq4000 technology. Sequencing data is available under GEO accession number GSE151618.

2.7 Transcriptomic analysis

Raw RNA-seq read sets were retrieved from the G enome Qu ebec's Nanuq portal, and pre-processed with BBDuk from the BBTools package (<https://sourceforge.net/projects/bbmap>) to trim sequencing adapters and remove reads derived from PhiX and ribosomal RNA. The transcriptome of *A. niger* NRRL3 (v. 20140311) was retrieved from the *jgi* Genome portal (Aguilar-Pontes et al., 2018), and the raw reads were mapped to the transcriptome using Salmon v0.14.1 (Patro et al., 2017). The libraries were imported in RStudio 1.2.5001 (RStudio: Integrated Development for R. RStudio, Inc., Boston, 2016) running R 3.6.1 (R Development Core Team 3.6.1., 2019) using tximport v.1.12.3 (Soneson et al., 2016). Differential gene expression was assessed

via pairwise comparisons using DESeq2 v1.24.0 (Love et al., 2014), using the design \sim mutation ($padj \leq 0.05$). Updated gene length data for the NRRL3 genome was retrieved from the *jgi* Genome portal. The full code is available at https://github.com/gabrifc/rnaseq_analysis_kexB.

2.8 Single gene knockouts of *kexB*

A deletion of *kexB* was introduced in the seven-fold *crh* knockout strain (TLF39) using a split marker approach. TLF39 (Table 1) was transformed after protoplastation as described previously (Arentshorst et al., 2012). Using the split marker approach for single gene knockouts, entire ORFs were deleted by replacement with the hygromycin B selection marker (Arentshorst et al., 2015). Flanks were generated via PCR using N402 genomic DNA as template and primers as described in Primer Table. *AOpyrG* fragments were obtained from plasmid pAN7-1 (Punt et al., 1987) with primers as described in Primer Table. Fusion PCR was used to generate split marker fragments containing *AOpyrG*. Approximately 2 μ g of DNA per flank was added to protoplasts for transformation. Transformation plates were incubated on MMS for 6 days at 30°C. Transformed colonies were single streaked on MM twice for purification and were genotyped using diagnostic PCR (data not shown).

2.9 Cell wall sensitivity assays

Cell wall disturbing compounds Calcofluor White (CFW), Congo Red (CR), Caspofungin (CA), sodium dodecyl sulfate (SDS, 0.004% and 0.005%), were added to MM plates. Spores were harvested as described above, counted, serially diluted into 2000, 200, 20 and 2 spores/ μ L and 5 μ L of respective dilutions were spotted on MM plates containing cell wall disturbing compounds. Plates were incubated for 3-5 days at 30°C.

3. RESULTS

3.1 Disruption of *kexB* shows a pH-dependent phenotype between pH 5.0 and pH 6.0 in fermenters

The deletion of *kexB* in *A. niger* is known to result in a pH dependent morphological phenotype on solid medium (Jalving et al., 2000). On pH 6.0 buffered agar plates, the Δ *kexB* strain displays a hyper-branching and compact phenotype whereas at pH 5.0 is growth like wild type (Jalving, 2005). To analyze the effect of the pH on the morphology during stirred submerged growth, we cultivated both parental strain (N402) and Δ *kexB* at pH 5.0, pH 5.5 and pH 6.0. Batch cultivations were performed at pH-controlled conditions using 0.75% glucose as carbon source. Dry weights were used to determine both the maximal specific growth rate (μ_{max}) and maximum biomass, which are listed in Table 2. At pH 5.0, both the growth rate ($0.200 \cdot h^{-1}$) and maximum biomass ($4.15 \text{ g}_{DW} \cdot \text{kg}^{-1}$) of the Δ *kexB* strain were found to be similar to the wild type ($0.187 \cdot h^{-1}$, $3.66 \text{ g}_{DW} \cdot \text{kg}^{-1}$). The hyphal morphology of the Δ *kexB* strain shows a wild type-like phenotype at pH 5.0, although the Δ *kexB* strain showed a slightly more open pellet morphology (Figure 1). Submerged growth at pH 5.5 showed slightly shorter hyphae and increased branching in case of the Δ *kexB*

strain compared to wild type, as can be seen in Figure 1. The growth rate and maximum acquired biomass at pH 5.5 for the $\Delta kexB$ strain ($0.194 \cdot h^{-1}$, $4.19 \text{ g}_{\text{DW}} \cdot \text{kg}^{-1}$) was similar to wild type ($0.175 \cdot h^{-1}$, $3.68 \text{ g}_{\text{DW}} \cdot \text{kg}^{-1}$) and also similar to the conditions at pH 5.0. When grown at pH 6.0, the $\Delta kexB$ strain again showed a similar growth rate ($0.211 \cdot h^{-1}$) and maximum biomass accumulation ($4.31 \text{ g}_{\text{DW}} \cdot \text{kg}^{-1}$) as at other pH conditions, but importantly, showed a very clear compact pellet phenotype (Figure 1). Cultivation of N402 at pH 6.0 resulted in severe biofilm formation on the walls of the fermenters. As a result, submerged biomass samples represented an incorrect measurement of both the submerged growth rate ($0.063 \cdot h^{-1}$) and amount of in-broth maximum biomass ($0.64 \text{ g}_{\text{DW}} \cdot \text{kg}^{-1}$). Microscopic analysis of the N402 pellets at pH 6.0 was similar hyphal morphology compared to pH 5.0 and pH 5.5. In general, base consumption to maintain the desired culture pH in all cultures was largely similar, as was also already published earlier for N402 (Niu et al., 2016).

Table 2. Growth parameters of wild type and $\Delta kexB$. Growth is shown as maximum growth rate per hour (μ_{max}) and maximum biomass ($\text{g}_{\text{DW}} \cdot \text{kg}^{-1}$) at different pH-controlled batch-cultivations.

pH condition	Wild type		$\Delta kexB$	
	$\mu_{\text{max}} (\text{h}^{-1})$	max biomass ($\text{g}_{\text{DW}} \cdot \text{kg}^{-1}$)	$\mu_{\text{max}} (\text{h}^{-1})$	max biomass ($\text{g}_{\text{DW}} \cdot \text{kg}^{-1}$)
pH 5.0	0.187	3.66	0.200	4.15
pH 5.5 (1)	0.175	3.68	0.194	4.19
pH 5.5 (2)	0.167	3.54	0.180	4.30
pH 6.0	0.063	0.64	0.211	4.31

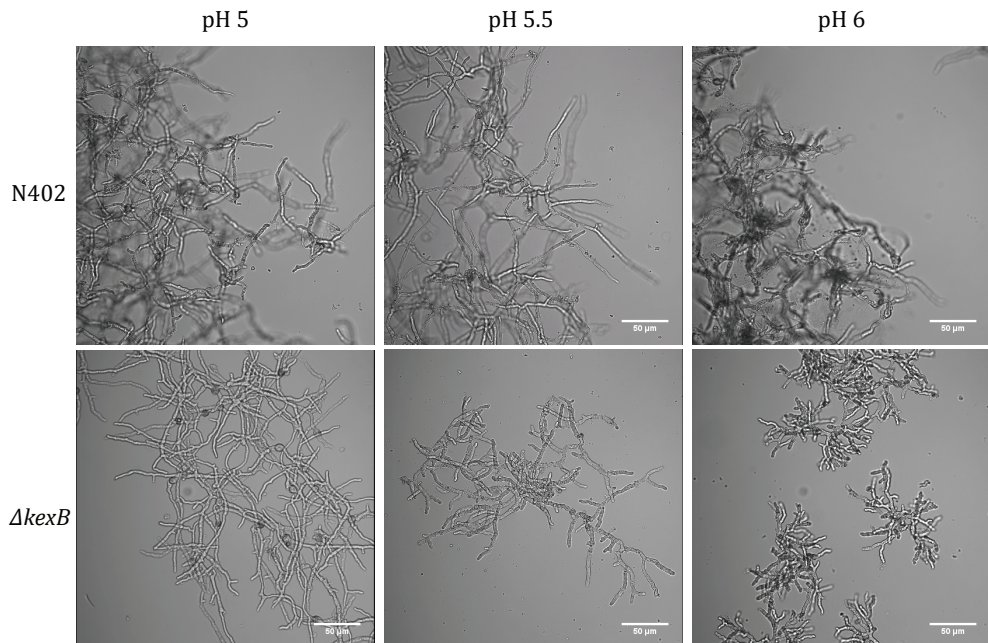
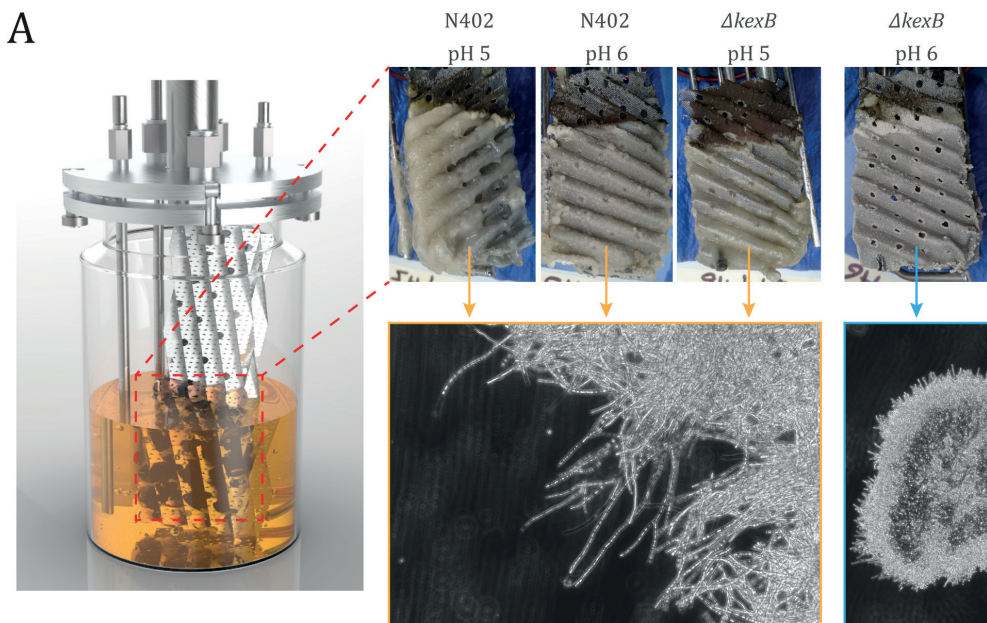


Figure 1. Pellet morphology of pH-controlled batch cultivations Wild type (N402) and $\Delta kexB$ strain microscopy samples taken at maximum biomass under different pH conditions: pH 5.0, pH 5.5 and pH 6.0.

3.2 Disruption of *kexB* displays reduced biofilm formation and more compact biofilm structure

As observed in the previous section, classical filamentous growth (i.e., without hyper-filamentation) displayed by wild type (N402) strain leads to severe biofilm proliferation on bioreactor walls. It seems thus that the hyper-filamentous phenotype exhibited by $\Delta kexB$ strain did not promote biofilm formation. In order to challenge this hypothesis, both strains have been cultivated in biofilm reactor at two different pH values (i.e., 5 and 6). This cultivation mode involves a standard lab-scale bioreactor where the mechanical stirring device has been removed and replaced by two sheets made of stainless-steel wire gauze (Figure 2A). This device has been evaluated for the cultivation of *Aspergillus oryzae* in a previous study and observations have pointed out the fact that fungal growth occurs exclusively on the metal sheets in this cultivation device (Zune et al., 2015), making the growth process fully dependent on the adhesion capacity of the strains. Qualitatively, wild type strain (N402) at both pH level and $\Delta kexB$ strain at pH 5 displayed similar biofilm morphologies, i.e. mycelium with relatively low ramification frequency. On the other hand, at pH 6 displayed a totally different biofilm morphology with, this one being composed of several hyper-ramified mycelial clumps instead of a continuous layer of mycelium (see microscopy images at figure 2A).

The two strains exhibited also differences at the quantitative level (Figure 2B), with biofilm dry weight for wild type strain (N402) cultivated at pH 5 and 6 were of 2.95 and 2.39 respectively (mean values), whereas mean dry weight of 1.74 and 1.31 respectively were observed for the $\Delta kexB$ strain. The pH-dependent hyper-filamentation phenotype of the $\Delta kexB$ strain is thus also observed in biofilm mode of cultivation, leading to reduced attachment on the metal supports and a much thicker biofilm structure with reduced water sorption capacity (Figure 2C).



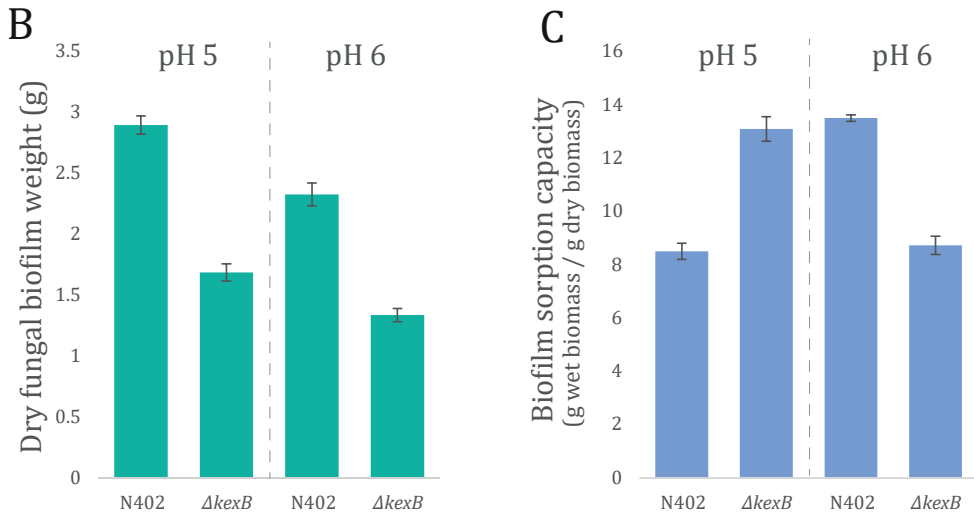


Figure 2. Submerged biofilm reactor cultivations of wild type (N402) and $\Delta kexB$. (A) Scheme of the biofilm reactor set-up used in this work and pictures displaying biofilm layer for each strain at two pH levels. Representative microscopy pictures (brightfield, 20x) are displayed for each type of biofilm structure. (B) Dry fungal biomass weight developed on the stainless-steel sheets in biofilm reactor and biofilm water sorption capacity (n = 2). Biofilm (water) sorption capacity is the difference between biofilm wet and dry weight.

3.3 Cell wall chitin content is increased in $\Delta kexB$ irrespective of morphology

To assess the relation of different hyphal branching morphologies at pH 5.0, pH 5.5 and pH 6.0 and cell wall chitin content, we isolated cell walls from maximum biomass samples that were obtained from bioreactor cultivations described above. Cell wall samples were hydrolyzed in triplicate and total glucosamine content was assessed using a colorimetric assay (section 2.5). Results of glucosamine measurements are shown in Figure 3. During all cultivations, the $\Delta kexB$ strain displayed an increase in chitin content compared to the wild type. The increase in percentage of cell wall glucosamine for the $\Delta kexB$ strain compared to the wild type were found to be $35.0 \pm 13.3\%$, $27.3 \pm 5.51\%$ and $29.6 \pm 6.62\%$ at pH 5.0, pH 5.5 and pH 6.0, respectively. Looking at absolute numbers of cell wall glucosamine per cell wall dry weight, we find that total glucosamine levels increase proportionally with the culture medium pH for both strains. Hence, cell wall glucosamine increases with increasing pH with about 20% between pH 5.0 and pH 6.0 and at all pH values the chitin content of the $\Delta kexB$ strain is about 30% higher compared the wild type.

3.4 Genome-wide expression profiling reveals changes in expression of cell wall biosynthetic genes

To gain better insight to transcriptomic responses in relation to cell wall biosynthetic changes occur as a result of lacking KexB, we decided to look into the transcriptome by performing RNA-sequencing on RNA extracted from wild type and the $\Delta kexB$ mutant grown at pH 5.5. A pH of

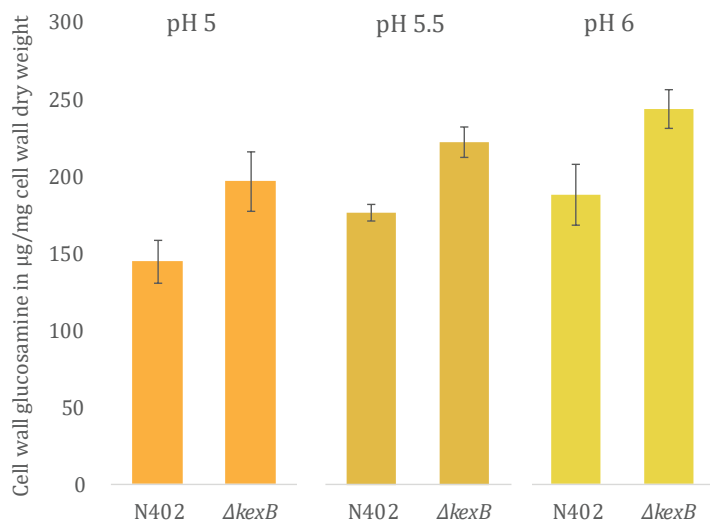


Figure 3. Cell wall glucosamine content of wild type (N402) and $\Delta kexB$ from pH-controlled batch cultivations. Cell wall glucosamine content maximum biomass samples that originate from single bioreactor cultivations, run at either pH 5.0, pH 5.5 (1) or pH 6.0. Measurements were performed in technical triplicates (n=3); error bars are the standard error (SE) and represent the variation of technical replicates.

5.5 resulted the most comparable growth conditions for both wild type and the $\Delta kexB$ strain. To obtain biological duplicates, additional bioreactor cultivations at pH 5.5 were performed and resulted in similar growth rates and maximum biomass accumulation as shown before for both wild type ($0.167 \cdot \text{h}^{-1}$, $3.54 \text{ g}_{\text{DW}} \cdot \text{kg}^{-1}$) and the $\Delta kexB$ strain ($0.180 \cdot \text{h}^{-1}$, $4.30 \text{ g}_{\text{DW}} \cdot \text{kg}^{-1}$) (Table 2). RNA was isolated from culture samples in the exponential growth phase at 90% of the maximum attained biomass. Duplicate batch-culture cultivations for both wild type and mutant were used to obtain a total of 4 RNA-sequencing samples. Following DeSeq2 analysis (section 2.7), we found 2461 transcripts (1163 up, 1298 down)—approximately 21% of the 11846 total transcripts—to be differentially expressed between the mutant strain and the wild type (adjusted p-value ≤ 0.05) (Expression data in Table S1).

For this study, we focused our interest to investigate to what extent cell wall biosynthesis was affected by deletion of *kexB*. To assess this, we checked for differential expression of all genes involved in 82 cell wall biosynthesis in *A. niger* as reported by Pel et al, 2007. Table 3 summarizes all cell wall related genes that were differentially expressed in the $\Delta kexB$ strain compared to N402. Differential expression was found for 29 out of 82 cell wall related genes involved in synthesis of all major components of the cell wall, including α -glucan, β -glucan and chitin, and the modification thereof (Table 3, Table S1, expression data). The results on increased cell wall chitin (Figure 3) were corroborated by transcriptional upregulation of gene encoding the rate limiting step in chitin precursor synthesis (UPD-*N*-acetylglucosamine), *gfaA* (FC 1.19) and *gfaB* (FC 6.22). Other genes involved in the synthesis of UPD-*N*-acetylglucosamine (*gnaA*, *pcmA* and *ugnA*) were not differentially expressed. Additionally, five chitin synthases were found to be upregulated in the $\Delta kexB$ strain (*chsB*, *chsC*, *chsD*, *chsE* and *chsG*), whereas four out of seven putative chitin-to-glucan crosslinking enzymes were found to be differentially expressed (*crhA*, and *crhD* upregulated; and *crhB* and *crhF* downregulated) along with four differentially expressed chitinases (*cfcD* and NRRL3_09653 upregulated; and *cfcG* and NRRL3_04221 downregulated).

Table 3. Differentially expressed cell wall biosynthesis genes in *Aspergillus niger*. 29 genes were differentially expressed (Padj ≤ 0.05) based on all 82 cell wall biosynthesis genes described by Pel et al., 2007.

CBS513.88 ID	NRRL3 ID	Gene description	Gene	Wild type (normalized read counts)	$\Delta kexB$ (normalized read counts)	FC	up or down regulated	Padj
α-glucan biosynthesis and modification								
An12g02460	NRRL3_09001	Putative GPI-anchored amylase-like protein (GH13-family) with possible function in alpha1,3-1,4-glucan processing	<i>agtB</i>	30	1114	38.06	up	1.43E-69
An12g02450	NRRL3_09002	Putative catalytic subunit alpha1,3-glucan synthase complex; SpAgs1-like	<i>agsC</i>	64	1688	26.48	up	5.91E-67
An04g09890	NRRL3_07454	Putative catalytic subunit alpha1,3-glucan synthase complex; SpAgs1-like	<i>agsA*</i>	104	574	5.52	up	8.90E-25
An08g09610	NRRL3_11494	Putative alpha-1,3-glucanase GH71; member of the SpAgn1-family	<i>agnD</i>	1496	6544	4.37	up	1.55E-71
β-glucan biosynthesis and modification								
An09g00670	NRRL3_00054	Predicted GPI-anchored protein. Putative 1,3- β -glucanosyltransferase GH72; member of the Gel-family	<i>gelD</i>	40	920	22.95	up	3.83E-73
An03g05290	NRRL3_08399	Predicted GPI-anchored protein. Putative beta-1,3-glucanosyltransferase GH17; member of the AfBgt1-family	<i>bgtB</i>	20956	29235	1.40	up	7.26E-04
An01g12450	NRRL3_02657	Putative exo-beta-1,3-glucanase (GH55-family); related to <i>Coniothyrium mitans</i> exo-1,3-glucanase (Cmg1)	<i>bxaA*</i>	4743	6407	1.35	up	8.95E-03
An06g01550	NRRL3_11624	Putative catalytic subunit beta1,3-glucan synthase complex; ScFks1-like	<i>fksA</i>	18189	23402	1.29	up	6.29E-04
An07g04650	NRRL3_04586	Putative beta-1,3-glucanosyltransferase GH17; member of the AfBgt1-family	<i>bgtC</i>	1161	847	-1.37	down	2.46E-03

Table 3. Differentially expressed cell wall biosynthesis genes in *Aspergillus niger*. 29 genes were differentially expressed (Padj ≤ 0.05) based on all 82 cell wall biosynthesis genes described by Pel et al., 2007. (Continued)

CBS513.88 ID	NRRL3 ID	Gene description	Gene	Wild type (normalized read counts)	$\Delta kexB$ (normalized read counts)	FC	up or down regulated	Padj
α-glucan biosynthesis and modification								
An10g00400	NRRL3_06317	Predicted GPI-anchored protein. Putative 1,3- β -glucanosyltransferase GH72; <i>A. fumigatus</i> Gel1-like	<i>gelA*</i>	14085	9570	-1.47	down	4.10E-08
An03g06220	NRRL3_08332	Predicted GPI-anchored protein. Putative 1,3- β -glucanosyltransferase GH72; member of the Gel-family	<i>gelE</i>	2008	192	-10.50	down	6.04E-120
An19g00090	NRRL3_01223	Putative exo-beta-1,3-glucanase (GH55-family); related to <i>Coniothyrium minitans</i> exo-1,3-glucanase (Cmg1)	<i>bgxC</i>	1101	102	-10.83	down	3.28E-50
Chitin biosynthesis and modification								
N/A	NRRL3_09653	Putative chitinase (N402 specific)	-	17	336	19.52	up	2.11E-17
An12g10380	NRRL3_02932	Putative chitin synthase ClassII; EnChsB-like	<i>chsE*</i>	3764	6517	1.73	up	1.35E-15
An08g05290	NRRL3_11152	Putative chitin synthase ClassVI;	<i>chsG</i>	147	252	1.71	up	4.56E-03
An14g00650	NRRL3_00641	Putative chitin synthase ClassI; EnChsC-like	<i>chsC</i>	2398	3814	1.59	up	2.44E-07
An14g00660	NRRL3_10021	Putative transglycosidase of GH16-family involved in cell wall biosynthesis; ScCrh1-like	<i>crhA</i>	737	1097	1.49	up	8.45E-04
An01g11010	NRRL3_02532	Predicted GPI-anchored protein. Putative transglycosidase of GH16-family involved in cell wall biosynthesis; member of the ScCrh1-family	<i>crhD*</i>	3637	5234	1.44	up	7.65E-04
An09g02290	NRRL3_00179	Putative chitin synthase ClassIV; EnChsD-like	<i>chsD</i>	2278	3104	1.36	up	1.99E-03
An09g04010	NRRL3_00331	Putative chitin synthase ClassIII; EnChsB-like	<i>chsB*</i>	6774	8553	1.26	up	5.98E-03
An01g05360	NRRL3_02063	Putative ClassV Chitinase (GH18); ScCts2-like	<i>cfcD</i>	1384	818	-1.69	down	3.96E-05

Table 3. Differentially expressed cell wall biosynthesis genes in *Aspergillus niger*. 29 genes were differentially expressed (Padj ≤ 0.05) based on all 82 cell wall biosynthesis genes described by Pel et al., 2007. (Continued)

CBS513.88 ID	NRRL3 ID	Gene description	Gene	Wild type (normalized read counts)	$\Delta kexB$ (normalized read counts)	FC	up or down regulated	Padj
Chitin biosynthesis and modification								
An16g02850	NRRL3_07085	Putative transglycosidase of GH16-family involved in cell wall biosynthesis; member of the ScCrh1-family	<i>crhF</i>	1468	812	-1.81	down	4.92E-08
An07g07530	NRRL3_04809	Predicted GPI-anchored protein. Putative transglycosidase of GH16-family involved in cell wall biosynthesis; ScCrh2-like	<i>crhB</i>	2205	988	-2.23	down	1.53E-09
N/A	NRRL3_04221	Putative chitinase (N402 specific)	-	174	58	-2.99		3.09E-03
An19g00100	NRRL3_01224	Putative ClassY Chitinase (GH18); ScCts2-like	<i>cfcG</i>	415	2	-197.88		8.05E-20
GH76 family proteins								
An11g01240	NRRL3_10041	Putative endo-mannanase (GH76-family) with a possible role in GPI-CWP incorporation; ScDfg5-like	<i>dfgH</i>	289	1103	3.82	up	2.58E-35
An14g03520	NRRL3_00897	Predicted GPI-anchored protein. Putative endo-mannanase (GH76-family) with a possible role in GPI-CWP incorporation; ScDfg5-like	<i>dfgC*</i>	1133	1996	1.76	up	6.95E-10
An16g08090	NRRL3_06700	Predicted GPI-anchored protein. Putative endo-mannanase (GH76-family) with a possible role in GPI-CWP incorporation; ScDfg5-like	<i>dfgE</i>	886	1169	1.32	up	2.14E-02
An02g02660	NRRL3_06048	Putative endo-mannanase (GH76-family) with a possible role in GPI-CWP incorporation; ScDfg5-like	<i>dfgG</i>	2587	1693	-1.53	down	3.75E-05

Table 3. Differentially expressed cell wall biosynthesis genes in *Aspergillus niger*. 29 genes were differentially expressed (Padj \leq 0.05) based on all 82 cell wall biosynthesis genes described by Pel et al., 2007. (Continued)

CBS513.88 ID	NRRL3 ID	Gene description	Gene	Wild type (normalized read counts)	$\Delta kexB$ (normalized read counts)	FC	up or down regulated	Padj
Rho-GAPs								
An18g06730	NRRL3_10703	Putative Cdc42-GTPase Activating protein (GAP) with similarity to ScBem3p	<i>capB</i>	1379	1783	1.29	up	5.54E-03
An13g00850	NRRL3_01500	Putative Rho1-GTPase Activating protein (GAP) with strong similarity to ScRgd2	<i>rapE</i>	2256	2755	1.22	up	1.91E-02
CWI signaling								
An04g10140	NRRL3_07436	Putative plasma membrane sensor required for cell wall integrity signaling; ScMtl1like	<i>mtlB</i>	93	575	6.16	up	6.51E-22
An07g04070	NRRL3_04545	Putative plasma membrane sensor-transducer of the stress-activated PKC1-MPK1 kinase pathway involved in maintenance of cell wall integrity; ScWsc1-like	<i>wscB*</i>	2073	2963	1.43	up	4.60E-05
An18g02400	NRRL3_10351	Protein kinase C with putative function in CWI signaling	<i>pkcA</i>	3602	4518	1.25	up	5.43E-03
An08g10670	NRRL3_11584	MAPK with putative function in Pheromone response/pseudohyphal growth pathway; ScFus3-like	<i>fusC</i>	2269	2808	1.24	up	1.39E-02

*Identified as induced upon cell wall stress (Meyer et al., 2007; Park et al., 2016)

Next to upregulation of chitin related transcripts, we observed the upregulation of *agsA* (FC 5.52), a gene known to be induced upon activation of the cell wall integrity (CWI) pathway in an RlmA dependent manner (Damveld et al., 2005). We checked for upregulation of additional genes involved in the CWI response, as previously published (Meyer et al., 2007; Park et al., 2016). Many of the reported genes were found to be represented in the differential dataset including *bxgA*, *gela*, *chsE*, *crhD*, *chsB*, *dfgC* and *wscB* (highlighted by asterisks in Table 3). However, some cell wall stress-related genes, such as chitin synthesis genes *gfaA* and *gfaB*, are not listed in this table. Taken together, the transcription data corroborate the observed increase in cell wall chitin and indicated that most of the CWI pathway is induced in a $\Delta kexB$ strain.

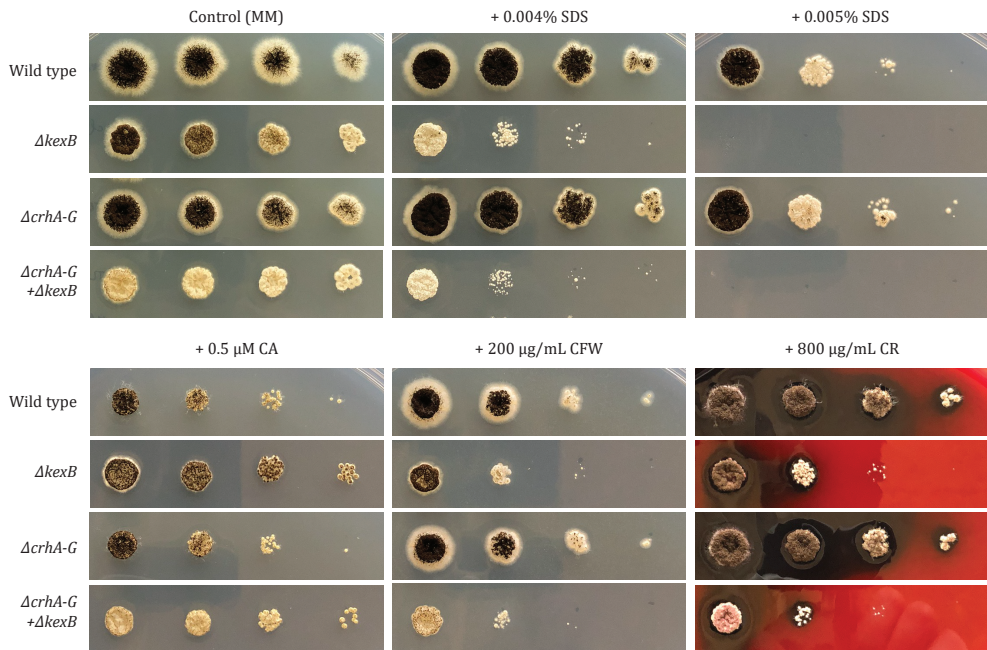


Figure 4. Susceptibility against cell wall disturbing compounds. Strains wild type (N402), $\Delta kexB$, $\Delta crhA-G$ and $\Delta crhA-G + \Delta kexB$ were grown on a cell wall sensitivity assay (section 2.9) using minimal medium (MM), pH 6.0 as base medium with additions of either SDS, Caspofungin (CA), CalcoFluor White (CFW) and Congo Red (CR). The number of spores plated, from left to right, are 10^4 , 10^3 , 10^2 and 10^1 spores, respectively. Strains were allowed to grow at 30°C for 96h prior to recordings, whereas the control was incubated for 65h.

3.5 Cell wall integrity is affected by disruption of *kexB*

To test whether a deletion of *kexB* affects the integrity of the cell wall, we exposed both the parental strain (N402) and $\Delta kexB$ to a series of cell wall disturbing compounds around pH 6.0 on plates—where the growth effect of $\Delta kexB$ is most prominent—that respond to changes in chitin content: Sodium dodecyl Sulfate (SDS), Caspofungin (CA), CalcoFluor White (CFW) and Congo Red (CR). As can be seen from Figure 4, the $\Delta kexB$ strain is more sensitive to SDS, CalcoFluor White (CFW) and Congo Red (CR) than the wild type, while slight resistance towards CA was observed for the $\Delta kexB$ strain in this assay.

In addition to an increase in chitin content for the $\Delta kexB$ strain, the transcriptional response showed differential expression for the majority of the chitin-to-glucan crosslinking *crh* family (Table 3). To investigate the importance of these enzymes in the construction and modification of existing chitin in the cell walls of the $\Delta kexB$ strain, we opted to knockout *kexB* in an existing seven-fold *crh* deletion (van Leeuwe et al., 2020c). We found that deleting *kexB* in the seven-fold *crh* deletion strain resulted sporulation deficiency. Despite the impact on sporulation, we neither observed a vegetative growth deficiency nor did we find a significant exacerbation of sensitivity towards any of the tested compounds when $\Delta crhA-G$ and $\Delta kexB$ were combined (Figure 4).

4. DISCUSSION

In this study we invoked the impact of deleting *kexB* in *A. niger* on hyphal morphology and cell wall composition by performing phenotypic, cell wall and transcriptomic analysis. We show that the characteristic hyper-branching pH-dependent phenotype of the $\Delta kexB$ strain, as reported on solid agar plates, is also prevalent in submerged solid support growth and submerged pH-controlled batch cultivations at pH 6.0. The phenotypic plasticity of the $\Delta kexB$ strain transitions between pH 5.0 and pH 6.0; pH-controlled conditions revealed that the $\Delta kexB$ strain morphology resembles wild type at pH 5.0, shows slightly shorter hyphae and smaller pellets at pH 5.5, and shows severe hyper-branching and tiny pellets at pH 6.0 (Figure 1). Despite the differences in morphology, both the growth rate and maximum biomass of the $\Delta kexB$ strain were not impaired and even slightly higher than the wild type across all pH conditions. It is interesting to note, however, that wild type growth at pH 6.0 resulted in severe biofilm formation at the fermenter walls whereas the $\Delta kexB$ strain did not.

To extend on the observation that *kexB* may be involved in surface attachment (i.e. biofilm formation), we grew both wild type and $\Delta kexB$ in specific biofilm reactors. Under these very specific cultivation conditions, it has been shown before that fungal growth occurs only on the metal sheets and not (or in very limited amount) in the liquid phase (Khalesi et al., 2014; Zune et al., 2015). On these metal sheets, the $\Delta kexB$ strain showed reduced biofilm formation compared to the wild type at both pH 5.0 and pH 6.0. These observations showed that a deletion of *kexB* limits the proliferation of the fungal biomass on the metal support. Additionally, we found that the hyper-branching phenotype of the $\Delta kexB$ strain was only observed at pH 6.0 and is very similar to the batch cultivation conditions at pH 6.0. Also, the biofilm of the $\Delta kexB$ strain produced at pH 6.0 is of a totally different structure than the one observed for the wild type, as well as for the $\Delta kexB$ strain at pH 5.0. This mycelial layer of hyper-branching phenotype growing on the metal support is more compact and displayed reduced water sorption capacity. It is important to take note that it remains unknown to what extent the morphology and biofilm composition will affect secretion and total production parameters and may be topics of future research. Despite these different mycelial properties of the hyper-branching morphology, a deletion of *kexB* reduced the ability to form biofilms at both pH conditions compared to the wild type. Furthermore, the increase in

pH from 5.0 and 6.0 appeared to affect both wild type and $\Delta kexB$ as a similar percentual drop in biofilm dry weight was observed between pH 5.0 and pH 6.0 (Figure 2B). Taken together, these data show that the *kexB* deletion shows a pH-dependent morphology at pH 6.0 without affecting growth rate or maximum biomass formation under submerged batch cultivation conditions. Additionally, the hyper-branching morphology showed less mycelial clumping and will reduce the stirring viscosity due to tinier pellets. As such, a deletion of *kexB* may provide a valuable industrial candidate strain for fermentation in near neutral pH conditions. Additionally, we observed that the *kexB* deletion resulted in visibly thicker cell walls that could be used as an added-value post-fermentation product.

Next, we investigated the cell wall composition of the $\Delta kexB$ strain and found an increase in cell wall chitin compared to the wild type; a trait that is often coupled to activation of the cell wall integrity to increase the strength of the cell wall (Fortwendel et al., 2010; Heilmann et al., 2013; Ram et al., 2004; van Leeuwe et al., 2020b, 2020a; Walker et al., 2015, 2008), and increased susceptibility towards CFW and resistance towards CA (Ram and Klis, 2006; Walker et al., 2015, 2013, 2008). The observed increase in chitin content from bioreactor cultivations was corroborated by the transcriptional upregulation of *gfaA*, and its paralogue *gfaB*, that are required for chitin precursor (UDP-*N*-acetylglucosamine) synthesis, known as the rate-limiting step for chitin synthesis (Lagorce et al., 2002; Ram et al., 2004). In addition, upregulation of multiple chitin synthases and downregulation of chitinases *cfcD*, *cfcG* and the N402 lineage-specific chitinase NRRL3_04221 were found. This transcriptional response is similar to that of the UDP-galactopyranose mutase A (*ugmA*) cell wall mutant, lacking cell wall galactofuranose, that also has increased cell wall chitin and chitin modifications by upregulation of *gfaA* and *gfaB*, *chsB* and *chsE* and severe downregulation of chitinase *ctcA* (Damveld et al., 2008; Park et al., 2016).

Aside from increased chitin synthesis in the $\Delta kexB$ strain, chitin-modifying enzymes also appear to play a role in the response to *KexB*-deficiency, as be inferred from the upregulation of *crhA* and *crhD*, and downregulation of *crhB* and *crhF* (Table 3). However, a combined deletion of all *crh* genes and *kexB* did not result in increased susceptibility to cell wall disturbing compounds. We did observe reduced sporulation, an effect that was also observed when a deletion of the seven-fold *crh* family and *ugmA* were combined (**Chapter 3**). In case of the *ugmA* strain, it has clearly been described that the CWI pathway is activated. Here, also the $\Delta kexB$ strain showed a large number of differentially expressed cell wall biosynthetic genes that are known to be upregulated during the CWI response. Moreover, the *kexB* deletion has been reported to induce the CWI response pathway by means of MAPK phosphorylation in *A. oryzae* and *A. fumigatus* (Mizutani et al., 2004; Te Biesebeke et al., 2005; Wang et al., 2015). In addition, the *Aspergillus oryzae kexB* (*AOkexB*) deletion has been reported to cause hyper-branching similar to *A. niger*, and increased amylase and protease production (Te Biesebeke et al., 2005). In *A. fumigatus*, a *kexB* deletion strain showed increased sensitivity towards CFW and CR, similar to our observations for the $\Delta kexB$ strain here (Figure 3). The sensitivity towards these compounds comined with the genome-wide expression profile confirm activation of the CWI pathway in $\Delta kexB$ strains.

The observed changes in cell wall chitin content in the *A. niger* $\Delta kexB$ strain are in congruence with *A. oryzae*, where a deletion of *kexB* was shown to increase cell wall chitin along with a reduction of α -glucan. This reduction in cell wall α -glucan was suggested to be caused by lack of KexB-processed α -glucan synthases (Mizutani et al., 2016). In this study, we did not analyze cell wall content for levels of α -glucan, however we did observe a very strong positive transcriptional response for both *agsA* (5.52 FC) and *agsC* (26.48 FC) in the $\Delta kexB$ strain. Similar to upregulation of chitin modifying enzymes, we found increased transcriptional expression of *agnD*, an alpha-1,3-glucanase (Meyer et al., 2009), and *agtB*, an α -glucan glycanosyl transferase (Levin et al., 2007; Yuan et al., 2008) in conjunction with the two α -glucan synthases. Upregulation of α -glucan metabolism may either indicate an attempted compensatory response to a lack of correctly processed α -glucan synthases (Yoshimi et al., 2017), or as a sign of general cell wall stress resulting from other improperly processed (cell wall) enzymes. Previously, we showed the relevance of proper α -glucan deposition in the cell wall for integrity; when α -glucan synthases *agsA* and *agsE* are disrupted in *A. niger* we showed that *crh*-facilitated chitin- β -glucan crosslinking genes become important for maintenance of cell wall integrity, while these genes are redundant when α -glucan synthesis is undisturbed (**Chapter 3**). Interestingly, α -glucan has also been described in relation to pathogenesis and hyphal aggregation for filamentous fungi (Yoshimi et al., 2017), by showing conidial and hyphal pellet clumping in α -glucan synthase knockouts of *A. fumigatus*, *A. oryzae* and *A. nidulans* (Henry et al., 2012; Miyazawa et al., 2018; Yoshimi et al., 2013). Hyphal aggregation of the *A. niger* $\Delta kexB$ strain appeared to be reduced across all three pH conditions (Figure 1) which may be related cell wall α -glucan levels. Further analysis of α -glucan dependent hyphal aggregation and biofilm formation may be a topic of future research.

Next to upregulation of α -glucan and chitin metabolism, *fksA*, the sole β -1,3-glucan synthase in *A. niger* was also found to be upregulated. Along with *fksA*, differential expression of glucanases and glucanosyltransferases (Table 2) were observed that are predicted to cause rearrangements of β -1,3-glucan polymer length and branching. This transcriptional response in *A. niger* is very similar to that observed in the *kexB* deletion in *A. fumigatus* that also resulted in upregulation of *gel* glucanosyltransferases (Wang et al., 2015), and results described on the β -1,3-glucan composition in *A. oryzae* where the *AO* $\Delta kexB$ strain showed a higher degree of β -glucan polymerization combined with slightly less branching (Mizutani et al., 2016). Together with the overall cell wall biosynthetic gene response, a deletion of *kexB* appears to bring about major cell wall content and compositional changes for all major constituents of the cell wall.

This study shows that the cell wall integrity of the $\Delta kexB$ strain is clearly affected, however without impairing growth rate or the maximally attained biomass during submerged batch cultivations. Contrarily, we did observe that *kexB* is important in formation of biofilms, as this mode of cultivation in biofilm reactors led to a reduction of the ability of to colonize the metal support. For now, understanding the characteristic phenotype of the $\Delta kexB$ strain during growth at pH 5.5 and 6 seems a consequence of pleiotropic effects of several hitherto unrelated responses. The morphology at pH 5.5/6.0 is possibly the result of loss of polarity due to the inability to synthesize

or modify the cell wall correctly. Many possible cell wall synthesis or cell wall modifying enzymes could be targets of KexB processing. Explanations for the pH-dependent effect have been postulated and suggest that at lower pH, other proteases can perform KexB-like dibasic processing (Jalving, 2005). In yeast, yapsins, aspartic proteolytic enzymes involved in processing cell wall proteins including Scw4p, Utr2p, Pir4p and Gas1p (Gagnon-Arsenault et al., 2008; Grbavac et al., 2017; Miller et al., 2010), show a pH dependent dependency to *kex2*. For Scw4p, it was shown that only at a neutral pH (7.0), but not at acidic pH (4.0), Kex2p is required for correct processing of the cell wall protein prior to yapsin processing, in order to activate the protein (Grbavac et al., 2017). It is likely that such a pH-dependent dependency on KexB may relationship of pro-protein processing that also exist in *A. niger*. Here, we showed that—despite the clear morphological changes in liquid between pH 5.0 and pH 6.0—the respective increase in cell wall chitin compared to wild type was observed across all pH conditions. From this we infer that the increase of chitin content is unlikely to dictate cell shape, however we cannot rule out chitin modifying enzymes to still play a role in the distinct phenotype. Taken together, the transcriptional data suggests activation of the CWI pathway that results in cell wall compositional rearrangements. Despite these findings, it remains to be elucidated how and if the KexB-dependent cell wall modifications are related to the pH dependent growth phenotype.

Acknowledgement

We would like to thank Prof. Dr. Bruno M. Moerschbacher for the coordination of the FunChi project.

Funding

This work is part of the “FunChi” ERA-IB project with project number ERA-IB-15-080, which is (partly) financed by the Dutch Research Council (NWO).

Availability of data and materials

The DNA reads described in this study will be deposited in the short read archive upon request. All other data are available on request by contacting Dr. Arthur F.J. Ram.

Supplemental information descriptions

Table S1. Expression data of differentially expressed genes. Includes a tab of expression levels of all cell wall biosynthetic genes, as described by Pel et al., 2007.

